MEDWIN PUBLISHERS
Committed to create value for Researchers

Nanomedicine & Nanotechnology Open Access
ISSN: 2574-187X

Self-Assembled O6-Succinyl Chitosan Nanoparticles for Controlled Release of Diosgenin and Agrochemicals

Quiñones JP[1]*, Kjems J[2], Yang C[2], Peniche C[3] and Brüggemann O[1]

[1]Institute of Polymer Chemistry, Johannes Kepler University Linz, Austria

[2]Department of Molecular Biology, Aarhus University, Denmark

[3]Center of Biomaterials, University of Havana, Cuba

Research Article

Volume 2 Issue 3

Received Date: October 31, 2017

Published Date: November 13, 2017

DOI: 10.23880/nnoa-16000128

***Corresponding author:** Javier Pérez Quiñones, Johannes Kepler University Linz, Institute of Polymer Chemistry, Altenberger Straße 69, 4040 Linz, Austria, Tel: +4368120399376; E-mail: javenator@gmail.com

Abstract

O6-succinyl chitosan was covalently linked to diosgenin and two synthetic brassinosteroid analogues with agrochemical and potential anticancer activity for their controlled release. FTIR and proton NMR spectroscopy confirmed functionalisation of chitosan matrix with the steroids. The prepared conjugates self-aggregated upon stirring and sonication in aqueous medium, as nanoparticles with 300 to 428 nm mean hydrodynamic diameters and steroid content between 5.8 and 13.4% (w/w). Scanning and transmission electron microscopy showed almost spherical 50-80 nm nanoparticles upon drying. Conjugates were also characterised by differential scanning calorimetry and wide-angle X-ray diffraction. In vitro steroid release studies performed in phosphate buffered saline solution at pH 6.0 indicated a drug release dependence on steroid content and hydrodynamic particles size. Almost constant release rates were observed for the first 8 hours and releases were extended for 96 hours. Brassinosteroid-modified nanoparticles showed better agrochemical activity in radish seeds bioassay than the parent brassinosteroids or O6-succinyl chitosan. The potential of these nanoparticles was also revealed by MMC cell proliferation bioassay and MB-MDA-231 cell cytotoxicity.

Keywords: O6-succinyl Chitosan; Controlled Release; Self-aggregated Nanoparticles; Steroids

Abbreviations: CS: Chitosan; DMF: Dimethylformamide; SCS: Succinyl Chitosan; PBS: Phosphate Buffered Saline Solution; TEM: Transmission Electron Microscopy; SEM: Scanning Electron Microscopy; DLS: Dynamic Light Scattering; WAXD: Wide-Angle X-ray Diffraction

Introduction

Chitosan (CS), a linear cationic polysaccharide composed by two β(1→4) linked monosaccharide residues, namely, N-acetyl-D-glucosamine and D-glucosamine, is a biopolymer obtained by extensive

deacetylation of chitin, a major component of arthropods, molluscs and crustacean exoskeleton, cell walls of fungi and cuticle of insects [1,2]. Several biomedical applications of chitosan related to its biocompatibility, biodegradability, bactericide, mucoadhesive, antifungal properties and low toxicity have been reported [3,4]. Additionally, chitosan promotes plant growth, stimulates nutrient uptake, increases germination of seeds and stimulates defense mechanisms in plants [5,6]. Some chitosan derivatives (i.e. N-succinyl chitosan, glycol chitosan, fructose chitosan) are preferred over chitosan and their conjugates because they exhibit superior water solubility and stability in aqueous solutions [7,8].

Brassinosteroids are plant hormones with steroidal structure widely found in the vegetal kingdom; in both reproductive and vegetative plant tissues [9]. Some natural brassinosteroids and synthetic brassinosteroid analogues are prepared for agrochemical, anticancer, antiherpetic and anti-HIV use in humans and animals [10,11]. On the other hand, diosgenin is usually employed as substrate in synthesis of some brassinosteroid analogues (i.e. DI31) because it is a cheap substrate with the required skeleton and stereochemistry; however diosgenin itself and some saponins containing it (i.e. dioscin, a natural saponin) exhibit important anticancer and antitumor activity [12,13]. Particularly, DI31 is a synthetic brassinosteroid analogue used as the commercial agrochemical Biobras-16 boosting the crops by 5 to 25% [14]. Though, exogenous brassinosteroid analogues are quickly metabolized in the plants and several foliar applications are needed before harvesting, with increased economic costs and environmental impact. A wisely engineered system for sustained agrochemical delivery would offer a better alternative to massive and repeated use of Biobras-16.

We have shown that with proper functionalisation of diosgenin and linking to chitosan it would be feasible to prepare pH-dependent delivery systems for the sustained release of agrochemicals and potential anticancer drugs [15]. However, these conjugates were not suitable for practical application because they showed low aqueous solubility at physiological conditions in plants and animals (30°C or 37°C, pH 7.0-7.4). Further synthesis and evaluation of N,O6-partially acetylated chitosan nanoparticles hydrophobically-modified for controlled release of diosgenin and the brassinosteroids was intended to overcome the limitations related to parent unmodified chitosans [16]. The high degree of acetylation achieved (DA 53%) in the prepared N,O6-partially acetylated chitosan nanoparticles reduced the high inherent surface charge of chitosan-based particles and inhibited totally the in vitro agrochemical activity of chitosan-linked brassinosteroids DI31 and S7 when evaluated at the concentrations employed in agriculture (10^{-6} to 10^{-7} mg mL^{-1}). That is why the design of other chitosan-based self-assembled particles for sustained delivery of agrochemicals is still under our research. The hypothesis of our work is that the advantages of carboxyl-containing chitosan over unmodified chitosan and hydrophobic acetylated chitosan for pH-controlled releases, would allow us to prepare suitable steroid-N-modified O6-succinyl chitosan nanoparticles with good agrochemical and potential anticancer activities. To the best of our knowledge the preparation of O6-succinyl chitosan covalently linked to steroids for their controlled release as agrochemicals and potential anticancer drugs has not been reported.

This article reports on preparation of self-aggregated nanoparticles of diosgenin- and two Cuban synthetic analogues of brassinosteroid-N-modified O6-succinyl chitosan, to achieve their controlled release.

Materials and Methods

The diosgenin and brassinosteroid analogues (DI31 and S7) employed to obtain the steroid hemisuccinates were kindly provided by the Center of Natural Products at University of Havana. Steroid hemisuccinates were synthesised by base-catalysed traditional esterification in pyridine with succinic anhydride [17]. Water soluble O6-succinyl chitosan was prepared by N-protection of commercial chitosan (acetylation degree, DA = 19.8% determined by ^{1}H-NMR, Mw= 4.3×10^{5}) as phthalimide chitosan, subsequent esterification with succinic anhydride in N,N-dimethylformamide (DMF) and deprotection with hydrazine monohydrate in DMF [18,19]. The solvents and reagents employed were purchased from Sigma-Aldrich and used without further purification.

The structures of O6-succinyl chitosan (SCS) and diosgenin hemisuccinyl O6-succinyl chitosan (SCS-MSD), DI31 hemisuccinyl O6-succinyl chitosan (SCS-MSDI31), S7 hemisuccinyl O6-succinyl chitosan (SCS-MSS7) conjugates are shown in Figure 1.

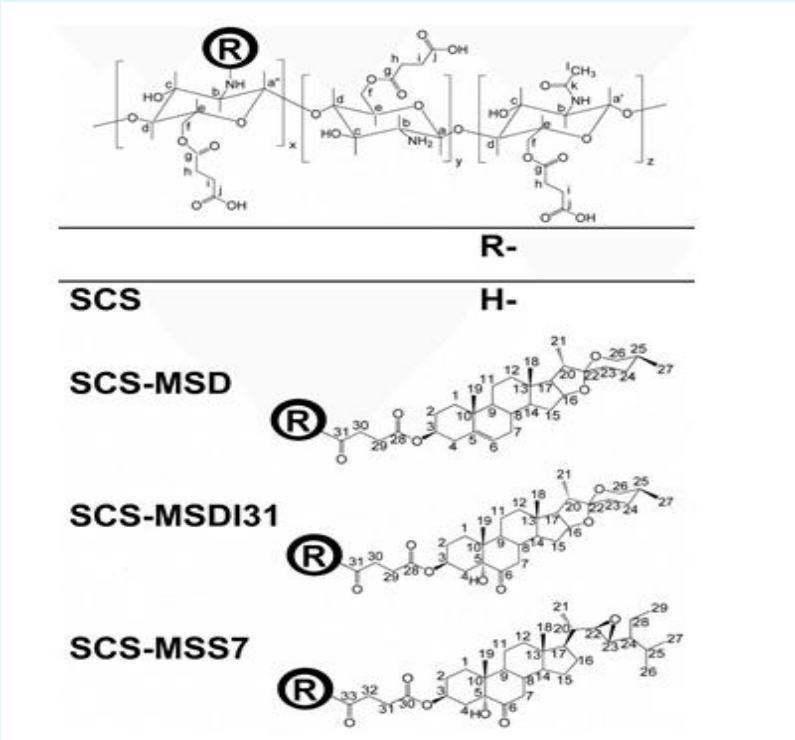

Figure 1: Structure of O6-succinyl chitosan (SCS) and diosgenin hemisuccinyl O6-succinyl chitosan (SCS-MSD), DI31 hemisuccinyl O6-succinyl chitosan (SCS-MSDI31), S7 hemisuccinyl O6-succinyl chitosan (SCS-MSS7) conjugates.

Synthesis of Steroid-N-Modified O6-Succinyl Chitosan Conjugates

100 mg (ca. 0.20 mmol) of steroid hemisuccinates were dissolved in 32 mL of ethanol/water solution (85:15, v/v). Then, 50 mg (0.26 mmol) of 1-ethyl-3-(3′-dimethylaminopropyl) carbodiimide hydrochloride and 30 mg (0.26 mmol) of N-hydroxisuccinimide were added and the mixture was stirred for 30 min at 0-4°C and for 2 hours at room temperature. The mixture was slowly added with stirring to a previously prepared O6-succinyl chitosan solution. To this end, 200 mg (ca. 0.7 mmol) of O6-succinyl chitosan were dissolved in 12 mL of double-distilled water and diluted with 36 mL of anhydrous ethanol. The reaction mixture was stirred at room temperature for 72 hours, dialyzed against ethanol/water mixtures (90:10, 66:33, 50:50, v/v) and double-distilled water (pH 7.0), each one for 2 days with 16 exchanges. These dialysed solutions were lyophilised affording white cotton wool-like products.

Preparation of the Self-Aggregated Nanoparticles

The steroid-N-modified O6-succinyl chitosan conjugates were able to form nanoparticles on aqueous medium after stirring overnight and probe tip sonication. To this end, the modified chitosan conjugates (ca. 0.5–2.0 mg mL^{-1}) were stirred overnight at 100 rpm in double-distilled water (pH 7.0) or phosphate buffered saline solution (PBS) at pH 7.4, as required. The solutions were probe tip sonicated (Branson Sonifier W-250) at 20 W for 2 min in an ice bath (0-4°C). The sonication step was repeated five times. The pulse function was pulsed on 8.0 s and pulsed off 2.0 s. This procedure is typically employed for self-assembly of amphiphilic chitosan-based materials as nanogel or nanoparticles in aqueous medium [8]. The obtained self-assembled SCS nanoparticles in aqueous medium were immediately employed for characterisation, release experiments and biological bioassays.

Characterisation of Steroid-N-Modified O6-Succinyl Chitosan Conjugates

The steroid-N-modified O6-succinyl chitosan conjugates were characterised by FTIR spectroscopy using a Perkin-Elmer FTIR spectrophotometer with 32 scans and 4 cm^{-1} resolution. Samples were prepared by the KBr pellet method. Elemental analysis was performed on a Varian MicroCube Analyzer with burning

temperature of 1150°C. The ^{1}H-NMR spectra were recorded with an OXFORD NMR AS400 (VARIAN) spectrometer operating at 400.46 MHz for proton at 25°C with concentrations ca. 25-8 mg mL^{-1} in d2-water and d4-methanol/d2-water (66%, v/v) for steroid-N-modified O6-succinyl chitosans or d4 acetic acid/d2-water (25%, v/v) for chitosan and analysed with the VNMRJ software, version 2.2 [8,20]. Wide-angle X-ray diffraction (WAXD) analysis of the powered samples was performed using a X'Pert MPD diffractometer (Philips, Holland) with Cu Kα radiation (40 kV, 30 mA, λ = 0.15418 nm), data collected at a scan rate of 1° min^{-1} with a scan angle from 4 to 50°. Calorimetric curves were obtained with a Perkin-Elmer Differential Scanning Calorimeter Pyris 1 and analysed with the Pyris 1 software (version 6.0.0.033). DSC studies were conducted using sample weights of approximately 5 mg, under a nitrogen dynamic flow of 20.0 mL min^{-1} and a heating-cooling rate of 10°C min^{-1} [21]. Samples were deposited in aluminium capsules and hermetically sealed. Indium was used to calibrate the instrument. Enthalpy (ΔH in J/g dry weight) and peak temperature were computed automatically. Samples were heated and cooled from -30 to 300°C.

Characterisation of Nanoparticles

Dynamic light scattering (DLS) studies were performed using a Zetasizer Nano ZS (Malvern Instruments, Malvern, UK) at 25°C to obtain the particle size and zeta potential. For zeta potential measurements nanoparticles were prepared in double-distilled water (pH 7.0) (ca. 1-2 mg mL^{-1}), while particle size measurements were conducted in PBS solution at pH 7.4 (ca. 0.5-1 mg mL^{-1}). The size and morphology of dried nanoparticles were studied by transmission electron microscopy (TEM) with a Philips CM20 operating at 200 kV and scanning electron microscopy (SEM) with a Nova NanoSEM 600 electron microscope. Each sample was stirred for 48 hours in double-distilled water (ca. 1 mg mL^{-1}), probe tip sonicated as already described and a drop of it was deposited on carbon plates. The excess solution was removed with filter paper and air-dried. The SEM samples were sputter-coated with gold. The TEM samples were negative stained with uranyl acetate solution (1%).

In Vitro Drug Release Studies

In vitro release of steroids from steroid-N-modified O6-succinyl chitosan nanoparticles was studied by UV detection (Genesys 10 UV–Vis Spectrophotometer, Thermo Spectronic, Rochester, NY, USA) at 280 nm (SCS-MSD), 300 nm (SCS-MSDI31), 300 nm (SCS-MSS7), respectively, at pH 6.0. To this end, 10–15 mg of steroid-N-modified O6-succinyl chitosan nanoparticles dissolved in 5 mL of PBS solution (pH 6.0) were placed in dialysis bags and dialysed against the release media (PBS, pH 6.0, 40 mL) at 37°C with constant agitation at 100 rpm. The entire media were removed at determined time intervals, and replaced with the same volume of fresh media. The amount of steroids released was determined by UV spectrophotometry and calculated from a previously obtained calibration curve (Figure 1 of supplementary materials and Table 1 of supplementary materials). These studies were conducted in triplicate for each sample.

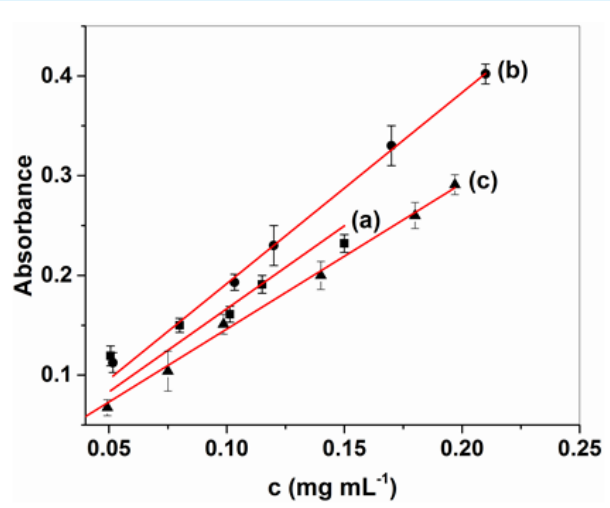

Figure 1: Supplementary materials. UV calibration curves of: (a) diosgenin, (b) DI31 and (c) S7 in PBS pH 6.0.

Samples	k (mL mg^{-1})	R^2
Diosgenin	1.66 ± 0.09	0.9866
DI31	1.92 ± 0.03	0.999
S7	1.46 ± 0.02	0.9991

Table 1: Supplementary materials. Linear fitting parameters of UV calibrations of steroids in PBS pH 6.0 (intercept 0, slope k, adjusted R-square R^2).

Cell Culture and Cytotoxicity

MB-MDA-231 cells (human breast cancer cell line) were maintained in DMEM (Invitrogen) media supplemented with 10% fetal bovine serum, 1% penicillin-streptomycin at 37°C in 5% CO_2 and 100% humidity. Murine Macrophage Cells (MMC) were cultured in RPMI 1640 media (Invitrogen) supplemented with 10% fetal bovine serum, 1% penicillin-streptomycin at 37 °C in 5% CO_2 and 100% humidity.

Cytotoxicity of all the samples were tested on both MB-MDA-231 and MMC cells by MTS assay (CellTiter 96® Aqueous One Solution Reagent). The cells in full growth media were seeded in 96-well plate (1 × 10^4 cells/well). After the cells attached on the plate, the media was changed to serum free media and steroids and steroid-N-modified O6-succinyl chitosan conjugates with different concentration were added. After incubation for 48 h, 20µL MTS reagent was added to each well and incubated for additional 3 hours before measuring the absorbance at 490 nm using a 96-well plate reader (µQuant, Bio-Tek Instruments Inc., USA).

Agrochemical Activity Radish Cotyledon Test

The radish (*Raphanus sativus*) cotyledons test was employed in order to detect plant growth activity. This bioassay consists of increased weight of the treated radish's cotyledons (auxin type activity). To this end, radish seeds previously sterilized by sodium hypochlorite treatment were germinated over wet filter paper in the dark at 25°C, for 72 h [22]. Cotyledons were separated of hypocotyls, weighted and treated with 5 mL of SCS-MSDI31 or SCS-MSS7 nanoparticles in water (10^{-1} to 10^{-7} mg mL^{-1}); DI31 or S7 solutions (10^{-1} mg mL^{-1} in ethanol/water solution 50% (v/v) and diluted up to 10^{-2} to 10^{-7} mg mL^{-1}); O6-succinyl chitosan aqueous solution (10^{-1} to 10^{-7} mg mL^{-1}) or pure water (control). After 72 h, cotyledons weights were measured. These studies were conducted in triplicate for each sample and concentration (10 cotyledons per each run).

Results and Discussion

The employed method afforded steroid-N-modified O6-succinyl chitosan conjugates with degree of substitution (DS, substituent per monosaccharide unit) of 0.041 (SCS-MSD), 0.065 (SCS-MSDI31) and 0.093 (SCS-MSS7); equivalent to weight contents of 5.8% (w/w) (diosgenin), 9.5% (w/w) (DI31) and 13.4% (w/w) (S7), respectively. The formation of the amides between the steroid hemisuccinates and O6-succinyl chitosan required mild conditions (stirring at room temperature, homogeneous reaction) and achieved yields of ca. 75%. The general trend of observed steroid reactivity with O6-succinyl chitosan was MSS7>MSDI31>MSD.

Characterisation of steroid-N-modified O6-succinyl chitosan conjugates

The FTIR spectra of chitosan, O6-succinyl chitosan and steroid-N-modified O6-succinyl chitosan conjugates are shown in Figure 2.

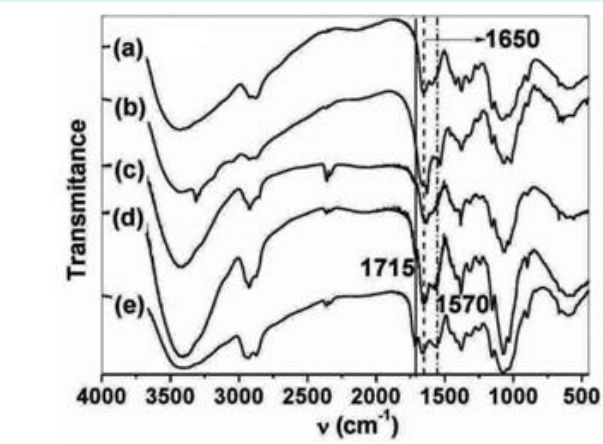

Figure 2: Infrared spectra of: (a) CS, (b) SCS, (c) SCS-MSD, (d) SCS-MSDI31 and (e) SCS-MSS7 (see Figure 1 for structures).

The IR spectrum of chitosan (Figure 2 (a)) presented characteristic absorption bands at 2942-2784 cm^{-1} (aliphatic C-H stretching band), 1658 cm^{-1} (Amide I) and 1597 cm^{-1} (-NH_2) bending and 1321 cm^{-1} (Amide III). Absorption bands observed at 1154 cm^{-1} (antisymmetric stretching of the C-O-C bridge), 1082 and 1032 cm^{-1} (skeletal vibrations involving the C-O stretching) are due to its saccharide structure [23].

O6-succinyl chitosan presents in addition to chitosan IR absorptions, a defined absorption band at 1634 cm^{-1} (C=O peaks of ester linkage).

The spectra of steroid-N-modified O6-succinyl chitosan conjugates are dominated by the intense and broad chitosan bands; however the C=O IR absorption of ester linkage is visible at 1662-1639 cm^{-1} (see Figure 2 (c)-(e)). These bands are overlapping the Amide I and -NH_2 ones at 1660-1652 cm^{-1} and 1597 cm^{-1}, producing a broad band ranging from 1700 to 1600 cm^{-1}. Also are observed intense IR absorption bands at 1560-1570 cm^{-1} and the increase in the Amide I band at 1654 cm^{-1}, as resulting of amide linkage between the O6-succinyl chitosan and steroid hemisuccinates (MSD, MSDI31 and MSS7). The characteristics C=O ketone band of the steroids are observed at 1715-1712 cm^{-1} (C6 at SCS-MSS7 and SCS-MSDI31).

Proton NMR spectrum of chitosan (Figure 2 (a) supplementary materials) showed characteristic peaks at 2.10 ppm (s, CH_3 of CH_3CO-), 3.19 ppm (s, 1H, H-2), 3.75 ppm (s, 1H, H-5), 3.80 ppm (s, 1H, H-6') and 3.90 ppm (s,

3H, H-6+H-4+H-3) as reported for crab chitosans [20]. O6-succinyl chitosan presented, in addition to proton peaks of chitosan, signals at 2.74 ppm (methylene groups, Hh + Hi of O6-succinyl chitosan succinic moiety); the lack of aromatic proton peaks (phthalimide group) is indicative of quantitative N-deprotection of SCS (Figure 2 (b) supplementary materials).

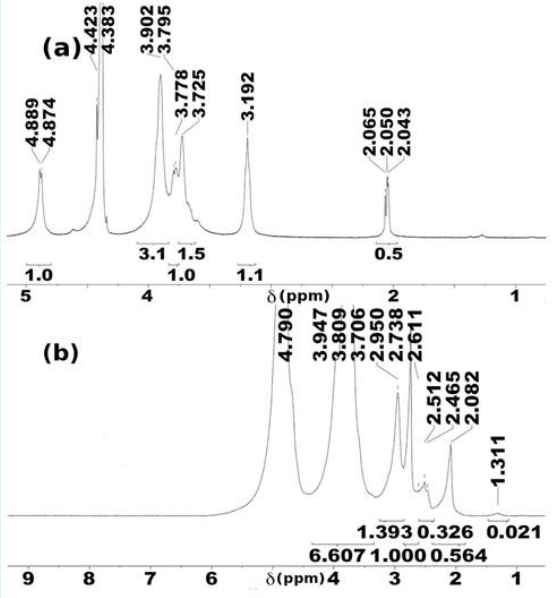

Figure 2 of supplementary materials. Proton NMR spectra of: (a) CS and (b) SCS at 8 mg mL^{-1} in D_2O at 25°C (see Figure 1 for structures).

The synthesised steroid-N-modified O6-succinyl chitosan conjugates formed self-aggregated nanoparticles in aqueous solution due to their hydrophilic/hydrophobic moieties (Scheme 1).

Scheme 1: Self-assembly of steroid-N-modified O6-succinyl chitosan conjugates dispersed in aqueous medium (water or PBS) as nanoaggregates after stirring overnight and probe tip sonication.

Their proton NMR spectra (Figure 3) presented the intense peaks of chitosan and additional peaks attributed to the steroid moiety. These peaks were observed at 0.71-1.05 ppm (methyl groups, H18 + H19 + H21 + H27 + H28), 1.33-1.35 ppm (methylene and methylidene groups, H1 + H9 to H17 + H20), 2.42-2.51 ppm and 2.84-2.85 ppm (methylene groups, H31 + H32 of succinyl moiety and Hh + Hi of O6-succinyl chitosan succinic moiety).

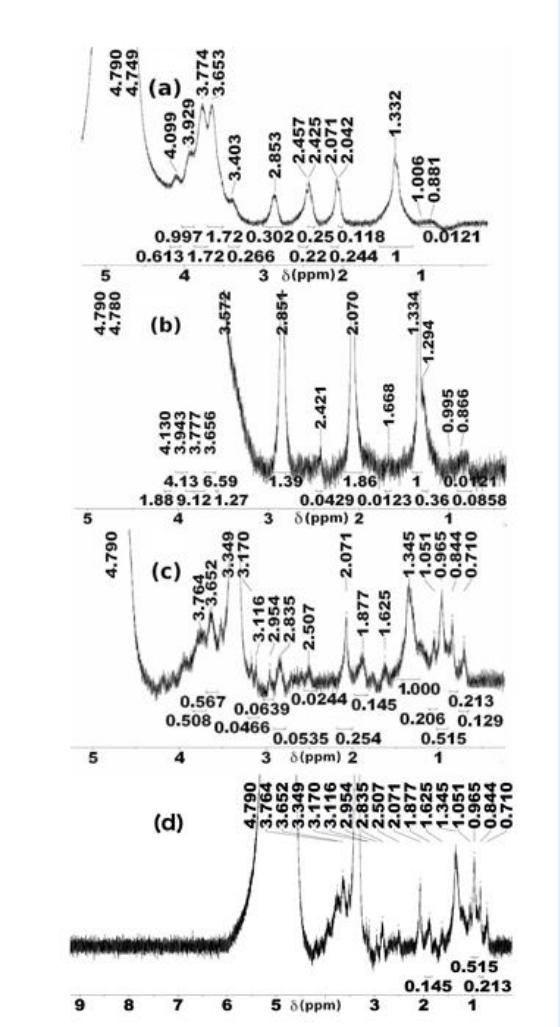

Figure 3: Proton NMR spectra of: (a) SCS-MSD, (b) SCS-MSDI31, (c) SCS-MSS7 and (d) SCS-MSS7 (range extended up to 9 ppm) at 8 mg mL^{-1} in CD_3OD/D_2O (2:1) at 25°C (see Figure 1 for structures).

The wide-angle X-ray diffraction patterns of chitosan, O6-succinyl chitosan and steroid-N-modified O6-succinyl chitosan conjugates are shown in Figure 4.

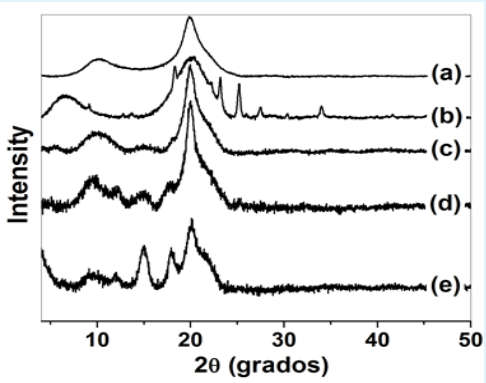

Figure 4: Wide-angle X-ray diffraction patterns of: (a) CS, (b) SCS, (c) SCS-MSD, (d) SCS-MSDI31 and (e) SCS-MSS7 (see Figure 1 for structures).

at 2θ 10.7 and 20.0° are observed (Figure 4 (a)). These peaks are attributed to the (020)h planes of the hydrated crystalline structure and the reflections of the hydrated polymorph, respectively [24]. These defined peaks are also observed in chitosans from crab shells [25]. On the other hand, O6-succinyl chitosan shows intense peaks between 2θ 6.7° and 25.2° (Figure 4 (b)); but the characteristic chitosan peaks are absent.

The steroid-N-modified O6-succinyl chitosan conjugates showed broad peaks between 2θ 4.0° and 25.1° (Figures 4(c)-(e)). The absence of intense peaks at 10.5-11.0° attributed to chitosan is indicative of its absence as crystalline phase. The characteristic narrow and intense peaks of pure steroid hemisuccinates were also absent (Table 2 of supplementary materials). Instead, several new peaks were observed, associated to the new crystalline phases of the obtained SCS conjugates.

Chitosan presented low crystallinity, but defined peaks

Samples	2 θ (degrees)								
MSD	11.0	15.0	15.6	15.9	17.6	18.4	21.5	21.7	22.9*
MSDI31	4.3	6.2*	8.6*	11.8	12.4	14.5	17.3	18.5	20.9*
MSS7	4.2	8.7	11.7	14.4	14.8	16.2	17.1	17.6	20.8
CS	10.7	20.0	-	-	-	-	-	-	-
SCS	6.5	9.1*	18.3	20.1	23.2	25.2	27.5*	30.3*	34.0*
SCS-MSD	5.4*	10.2	15.1*	20.0	-	-	-	-	-
SCS-MSDI31	9.5	12.1	15.2	17.8	20.0	25.1*	-	-	-
SCS-MSS7	4.0	9.5*	12.0*	15.0	17.9	20.1	-	-	-

* Stands for peaks of low intensity.

Table 2: Supplementary materials. WAXD peaks of steroid hemisuccinates, chitosan, O6-succinyl chitosan and steroid-N-modified O6-succinyl chitosan conjugates (see Figure 1 for structures).

The DSC curves of chitosan, O6-succinyl chitosan and steroid-N-modified O6-succinyl chitosan conjugates are shown in Figure 5.

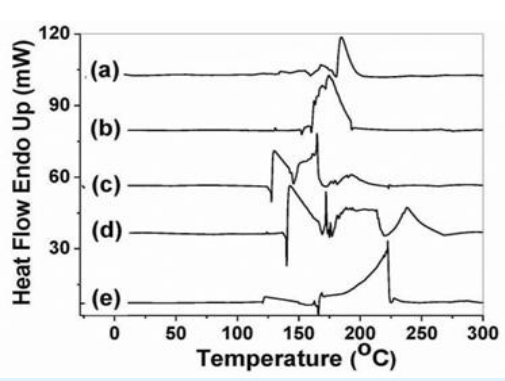

Figure 5: DSC Curves of: (a) CS, (b) SCS, (c) SCS-MSD, (d) SCS-MSDI31 and (e) SCS-MSS7 (see Figure 1 for structures).

The DSC of chitosan placebo (Figure 5(a)) showed two endothermic peaks at 170.4°C and 187.0°C, respectively. The total ΔH of these effects is 124.1 J/g. These endothermic effects result mainly from the melting and dissociation of chitosan crystals, by comparison with crab chitosans [23]. The DSC of O6-succinyl chitosan (Figure 5(b)) shows an intense endothermic peak at 175.0°C with associated ΔH of 165.6 J/g (see Table 3 of supplementary materials). Therefore, melting of SCS crystals and dissociation of the polymer chains occur at similar temperatures and require similar energy (ΔH). The DSC of steroid-N-modified O6-succinyl chitosan conjugates (Figures 5(c)-(e)) showed intense endothermic peaks between 130-238°C with associated ΔH between 44–7650 J/g (Table 3 of supplementary materials). These peaks might be due to the melting of SCS functionalized with the steroids, dissociation and decomposition of steroid-N-modified O6-succinyl chitosan chains. The high energies

related to the melting and dissociation of SCS conjugate chains might be due to the hydrophobic interactions of steroid linked to different SCS chains.

Samples	Endotherm (°C)			
	Onset	Peak	Completion	ΔH (J/g)
CS	167.2	170.4	174.1	3.5
	181.5	187.0	197.8	120.6
SCS	171.6	175.0	192.1	165.6
SCS-MSD	127.8	129.9	146.4	1045.1
	146.4	166.5	174.8	1247.5
SCS-MSDI31	136.9	139.5	159.6	2188.7
	167.7	170.1	171.8	142.8
	173.2	173.8	175.4	43.6
	175.4	212.5	218.7	3368.0
	218.7	237.5	254.3	1311.5
SCS-MSS7	119.5	121.9	149.6	673.5
	153.9	161.9	163.3	290.4
	165.0	167.8	169.6	223.4
	169.6	222.1	224.4	7649.7

Table 3: Supplementary materials. Thermal properties and main thermal effects of chitosan, O6-succinyl chitosan and steroid-N-modified O6-succinyl chitosan conjugates (see Figure 1 for structures).

Characterization of Steroid-N-Modified O6-Succinyl Chitosan Nanoparticles

Dynamic light scattering studies revealed average hydrodynamic particle diameters in PBS (pH 7.4) of 304 ± 2 nm with a polydispersity index (PDI, related to the width of the overall distribution) of 0.254 ± 0.002 (SCS-MSD), 300 ± 2 nm with a PDI of 0.32 ± 0.04 (SCS-MSDI31) and 428 ± 4 nm with a PDI of 0.47 ± 0.05 (SCS-MSS7). These nanoparticles were accompanied by ca. 2-6 mol % aggregates of 4.2-6.3 μm. Zeta potential measurements in double-distilled water ranged from 27 ± 1 mV (SCS-MSD), 35 ± 2 mV (SCS-MSDI31) to 23.5 ± 0.5 mV (SCS-MSS7). These positive zeta potential values are attributed to the cationic ammonium groups of chitosan moieties on the surface of SCS nanoparticles. The high zeta potential values (ca. to 30 mV) related to high surface charges of the prepared SCS nanoparticles, might explain the observed colloidal stability in aqueous medium. Thus, no sedimentation of the SCS particle aqueous dispersions was observed after 10 days of storage (no significant differences in hydrodynamic diameters and PDI, data not shown).

SEM and TEM images of dried steroid-N-modified O6-succinyl chitosan nanoparticles showed almost spherical shaped particles with 50-80 nm mean diameters (Figure 6). The drying and dehydration processes of steroid-N-modified SCS nanoparticles before the electron microscopy imaging caused a shrinkage of ca. 70 to 80%, similarly to the observed in other chitosan-based conjugates [16,26].

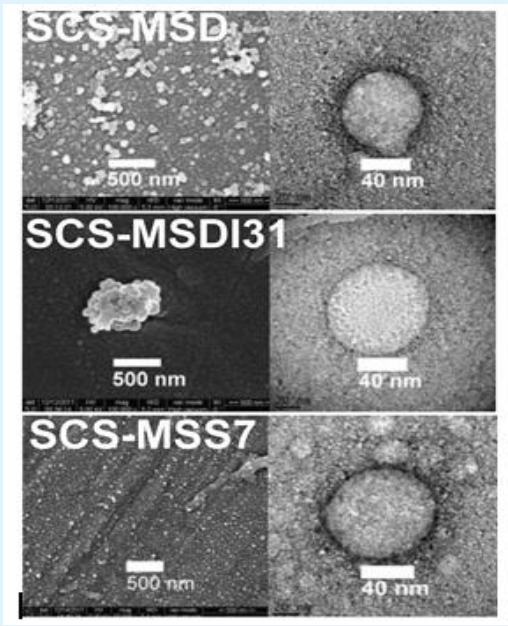

Figure 6: Scanning electron micrographs of SCS-MSD, SCS-MSDI31 and SCS-MSS7 nanoparticles at 100,000X magnifications (scale bar: 500 nm); transmission electron micrographs at 100,000X magnifications (scale bar: 40 nm) with negative staining with 1% uranyl acetate (see Figure 1 for structures).

Drug Delivery

A preliminary release experiment of the ester hydrolysis against pH was performed to assess the kinetic of steroid release from the steroid-N-modified O6-succinyl chitosan nanoparticles at 30°C and 37°C (Table 4 of supplementary materials). It was observed a faster steroid release with a pH reduction and with a temperature increase, related to an enhanced ester hydrolysis at lower pH and higher temperature. However, it is known that the cancer tissues are slightly acidic (pH ca. 6.5) due to augmented excretion of lactic acid from enhanced glucose metabolism in the cancer cells [27], and uptake of foreign bodies by endocytosis might bring the SCS nanoparticles to lysosomes with a lower pH of 5.0 [28]. Besides, the vacuoles in plant cells also possess a pH ca. 6.0 and some hydrolytic enzymes (i.e. esterases, chitosanases) capable to degrade the SCS nanoparticles that entered via endocytic uptake, hence liberating the applied brassinosteroids in the plants [29]. That is why the in vitro drug release experiments were conducted at pH 6.0. Figure 7 shows the in vitro steroid release profiles at 37 ± 2°C in PBS solution (pH 6.0), expressed as percentage steroid cumulative release against time from steroid-N-modified O6-succinyl chitosan nanoparticles.

Temperature	pH 7.4	pH 6.0	pH 4.0	pH 2.0
30 °C	N.O.	6 ± 3	17 ± 4	31 ± 5
37 °C	< 5	12 ± 5	29 ± 3	43 ± 4

N.O. stands for not observed

Table 4: Supplementary materials. Percentage (%) of diosgenin released after 4 hours from SCS-MSD nanoparticles at different pH and temperatures (see Figure 1 for structures).

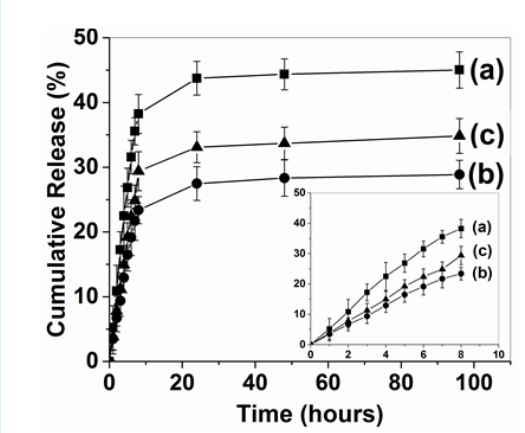

Figure 7: In vitro release profiles of: (a) SCS-MSD, (b) SCS-MSDI31 and (c) SCS-MSS7 in PBS (pH = 6.0) at 37°C. Data are the mean ± standard deviation (n = 3) (see Figure 1 for structures).

The studied steroids were delivered with almost constant release rate (zero order kinetics) during the first 8 h from the steroid-N-modified O6-succinyl chitosan nanoparticles. These releases appeared not quantitative and dependent on the steroid content and the hydrated particle sizes in PBS, reaching 45% (SCS-MSD), 29% (SCS-MSDI31) and 35% (SCS-MSS7), respectively after 96 h. Thus, particles with the lowest steroid content (SCS-MSD) released fastest and more quantity of the covalently linked steroid; while the bigger particles of SCS-MSS7, with a 3% more in steroid content than SCS-MSDI31, showed a faster release profile than the SCS-MSDI31 nanoparticles. The significant quantities of steroid released at slightly acidic pH (pH 6.0) after 8 hours might be due to the periodic replacement of full release medium with the fresh one every 1 hour. A frequent removal of ester hydrolysis products from the system should increase significantly the rate of hydrolysis at pH 6.0. Thus, it is observed in Figure 7(a) that the percentage of diosgenin released at 4 hours is ca. 23 %, a doubled quantity of the steroid released at same time without previous replacements of the release medium (Table 4 of supplementary materials). On the other hand, the unreleased steroid linked to chitosan matrix might be available after partial enzymatic degradation of SCS nanoparticles inside vegetal cells.

Agrochemical Activity

Figure 8 shows the plant growth biological activity of the synthetic brassinosteroids, O6-succinyl chitosan and brassinosteroid-N-modified O6-succinyl chitosan nanoparticles in the radish cotyledons bioassay.

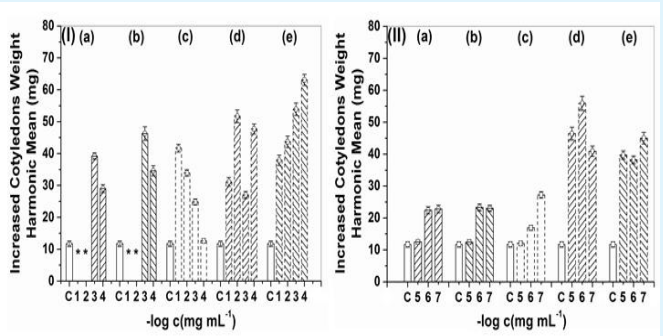

Figure 8: Biological activity as plant growth regulator of (I): (a) DI31, (b) S7, (c) SCS, (d) SCS-MSDI31 and (e) SCS-MSS7 at control (C) and 10^{-1} to 10^{-4} mg mL^{-1} at 25°C; (II): (a) DI31, (b) S7, (c) SCS, (d) SCS-MSDI31 and (e) SCS-MSS7 at control (C) and 10^{-5} to 10^{-7} mg mL^{-1} at 25°C . (*) Not measured because cotyledons died as result of high ethanol content. Data are the mean ± standard deviation (n = 3) (see Figure 1 for structures).

Plant growth stimulator activities of the synthetic brassinosteroids DI31 and S7 are similar, with best results at 10^{-3} and 10^{-4} mg mL^{-1} concentrations, but almost a doubled cotyledons weight was reached as compared to control with the lowest concentrations (10^{-6} and 10^{-7} mg mL^{-1}). O6-succinyl chitosan exerts a growth stimulator effect at high (10^{-1} to 10^{-4} mg mL^{-1}) and at low concentrations (10^{-6} to 10^{-7} mg mL^{-1}), as expected of the stimulatory effect reported for crab chitosans [5,30].

The SCS-MSDI31 and SCS-MSS7 nanoparticles in aqueous medium exhibited stimulatory plant growth activities at the studied concentrations (10^{-1} to 10^{-7} mg mL^{-1}), especially at medium and low concentrations (10^{-5} to 10^{-7} mg mL^{-1}) (weight increased approximately three or five times compared to control and two times compared with same concentration of parent brassinosteroids or O6-succinyl chitosan). These results are very promising for a practical agrochemical application of these compounds (the pure DI31 and S7 brassinosteroids are usually applied at concentrations of 10^{-5} to 10^{-7} mg mL^{-1} in agriculture). The higher agrochemical activity of brassinosteroid-N-modified SCS conjugates as compared to parent DI31, S7 and SCS might be due to the sustained delivery of the brassinosteroids in the required nanomolar concentrations for optimal impact in vegetal metabolism and regulatory mechanisms [31] and to a synergy as plant growth stimulator of SCS and the brassinosteroids.

Cell Proliferation and Cytotoxic Activity

Figure 3 of supplementary materials shows the relative cell viability of MMC cells at different concentrations of steroid-N-modified O6-succinyl chitosan nanoparticles and parent steroids. The MMC cell viability resulted almost unaffected as a result of treatment with the steroid-N-modified O6-succinyl nanoparticles and parent steroids. Thus, it seems that the parent steroids and the synthesised SCS conjugates are harmless to normal cells (no cancer cells, i.e. MMC). However, further studies are required to properly assess the toxicity of studied steroids and SCS conjugates.

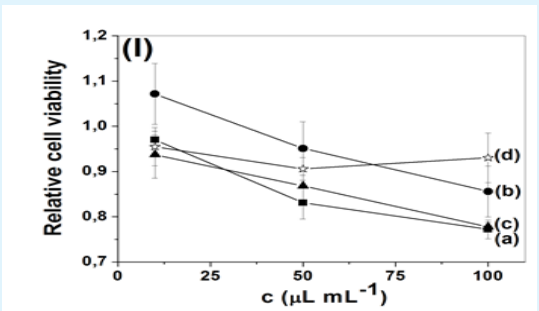

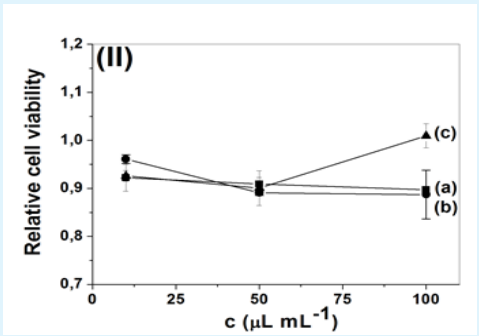

Figure 3 of supplementary materials. MCC MTS-based relative cell viability of: (I) (a) diosgenin, (b) DI31, (c) S7 and (d) SCS; (II) (a) SCS-MSD, (b) SCS-MSDI31 and (c) SCS-MSS7 (see Figure 1 for structures).

Figure 4 of supplementary materials presents the relative cell viability of MB-MDA-231 cells at different concentrations of the steroid-N-modified O6-succinyl chitosan nanoparticles and parent steroids. The obtained steroid-N-modified O6-succinyl chitosan nanoparticles seemed slightly more cytotoxic to the MB-MDA-231 cell line than the parent steroids at the studied concentrations. These results endorse a potential application of the synthesised steroid-N-modified O6-succinyl chitosan nanoparticles as a drug delivery system for anticancer therapy, but further studies are required.

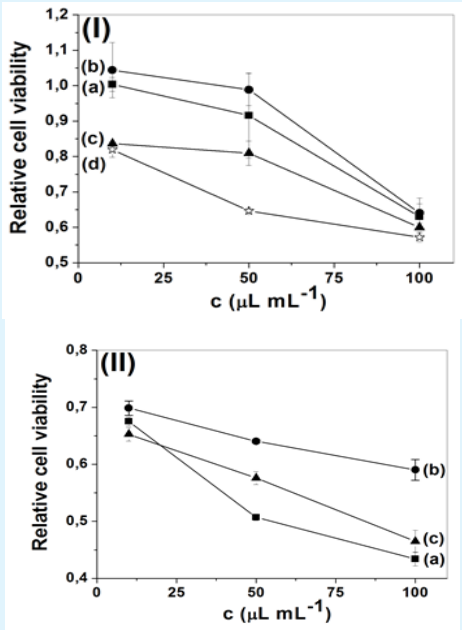

Figure 4 of supplementary materials. MB-MDA-231 MTS-based relative cell viability of: (I) (a) diosgenin, (b) DI31, (c) S7 and (d) SCS; (II) (a) SCS-MSD, (b) SCS-MSDI31 and (c) SCS-MSS7 (Figure 1 for structures).

Conclusion

In this research, three steroid-N-modified O6-succinyl chitosan conjugates were synthesised for controlled release of agrochemicals and potential anticancer drugs, as confirmed by FTIR and proton NMR spectroscopy. These conjugates were able to self-aggregate forming nanoparticles in aqueous medium upon stirring and probe tip sonication. In vitro release studies performed in PBS (pH 6.0) indicated a drug release dependence on steroid content and hydrodynamic particle sizes. Almost constant release rates were observed during the first 8 h. Brassinosteroid-N-modified O6-succinyl chitosan nanoparticles showed better plant growth stimulatory activity than parent brassinosteroids and O6-succinyl chitosan in radish seeds bioassay at low concentrations of 10^{-5} to 10^{-7} mg mL^{-1}. The potential of these nanoparticles for anticancer treatments was also explored based on MMC cell proliferation and MB-MDA-231 cell cytotoxicity.

Acknowledgement

The authors wish to thank the Erasmus Mundus foundation for a research grant to Javier Pérez Quiñones. Prof. Jacques Chevallier and Ms. Karen E. Thomsen are acknowledged for electron microscopy measurements at Aarhus University, Denmark. Prof. Jens-Erik Jørgensen is acknowledged for X-ray diffraction measurements in Department of Chemistry, Aarhus University, Denmark. Prof. Dr. Claudia Schmidt is gratefully acknowledged for helpful revision of the manuscript and elemental analysis and DSC measurements in the Department of Chemistry, University of Paderborn, Germany.

Conflicts of Interest

Authors declare that we have no conflict of interest on submission of manuscript for publication.

References

1. Muzzarelli RAA (2009) Chitins and chitosans for the repair of wounded skin, nerve, cartilage and bone. Carbohydrate Polymers 76(2): 167-182.

2. Shukla SK, Mishra AK, Arotiba OA, Mamba BB (2013) Chitosan-based nanomaterials: A state-of-the-art review. Int J Biol Macromol 59: 46-58.

3. Fernandez JG, Seetharam S, Ding C, Feliz J, Doherty E, et al. (2017) Direct Bonding of Chitosan Biomaterials to Tissues Using Transglutaminase for Surgical Repair or Device Implantation. Tissue Eng Part A 23(3-4): 135-142.

4. Muzzarelli RAA, Boudrant J, Meyer D, Manno N, De Marchis M, et al. (2012) Current views on fungal chitin/chitosan, human chitinases, food preservation, glucans, pectins and inulin: A tribute to Henri Braconnot, precursor of the carbohydrate polymers science, on the chitin bicentennial. Carbohydrate Polymers 87: 995-1012.

5. Malerba M, Cerana R (2016) Chitosan Effects on Plant Systems. Int J Mol Sci 17(7): 996-1011.

6. Mukta JA, Rahman M, Sabir AA, Gupta DR, Zahan S, et al. (2017) Chitosan and plant probiotics application enhance growth and yield of strawberry. Biocatalysis and Agricultural Biotechnology 11: 9-18.

7. Yan C, Chen D, Gu J, Hu H, Zhao X, et al. (2006) Preparation of N-Succinyl-chitosan and Their Physical-Chemical Properties as a Novel Excipient. Yakugaku Zasshi 126(9): 789-793.

8. Jing Mou Y, Li Yan Q, Yi J, Yong Jie L (2008) Self-aggregated nanoparticles of cholesterol-modified glycol chitosan conjugate: Preparation, characterization, and preliminary assessment as a new drug delivery carrier. European Polymer Journal 44: 555-565.

9. Tang J, Han Z, Chai J (2016) Q&A: what are brassinosteroids and how do they act in plants. BMC Biology 14: 113-118.

10. Duran MI, González C, Acosta A, Olea AF, Díaz K, et al. (2017) Synthesis of Five Known Brassinosteroid Analogs from Hyodeoxicholic Acid and Their Activities as Plant-Growth Regulators. Int J Mol Sci 18(3): 516-529.

11. Khripachb VA, Mehtieva AR, Misharina AY, Timofeevc VP, Tkachev YV, et al. (2010) Toxicity of (22R,23R)-22,23-dihydroxystigmastane derivatives to cultured cancer cells. Steroids 75(3): 287-294.

12. Fernández PP, Hui KM, Li F, Rajendran P, Sethi G (2010) Diosgenin, a steroidal saponin, inhibits STAT3 signaling pathway leading to suppression of proliferation and chemosensitization of human hepatocellular carcinoma cells. Cancer Lett 292(2): 197-207.

13. Tong Q, Quing Y, Wu Y, Hu X, Jiang L, et al. (2014) Dioscin inhibits colon tumor growth and tumor angiogenesis through regulating VEGFR2 and AKT/MAPK signaling pathways. Toxicol Appl Pharmacol 281(2): 166-173.

14. Serrano YC, Fernández RR, Pineda FR, Pelegrín LTS, Fernández DG, et al. (2015) Synergistic effect of low doses of X-rays and Biobras-16 on yield and its components in tomato (*Solanum lycopersicum L.*) plants. American Journal of Bioscience and Bioengineering 3: 197-202.

15. Quiñones JP, Szopko R, Schmidt C, Covas CP (2011) Novel drug delivery systems: Chitosan conjugates covalently attached to steroids with potential anticancer and agrochemical activity. Carbohydrate Polymers 84: 858-864.

16. Quiñones JP, Gothelf KV, Kjems J, Caballero AMH, Schmidt C, et al. (2013) Self-assembled nanoparticles of modified-chitosan conjugates for the sustained release of DL-α-tocopherol. Carbohydr Polym 92(1): 856-864.

17. Abe T, Hasunuma K, Kurokawa M (1976) Vitamin E orotate and a method of producing the same. US: 3944550.

18. Fang Y, Huang M (2006) Facile preparation of biodegradable chitosan derivative having poly(butylene glycol adipate) side chains. Biopolymers 82(6): 597-602.

19. Shen J, Ping Q, Zhang C, Zhang H (2003) Synthesis and characterization of water-soluble O-succinyl-chitosan. European Polymer Journal 39: 1629-1634.

20. Berrada M, Buschmann MD, Gupta A, Lavertu M, Rodrigues A, et al. (2003) A validated 1H NMR method for the determination of the degree of deacetylation of chitosan. Journal of Pharmaceutical and Biomedical Analysis 32: 1149-1158.

21. Basaran E, Yazan Y, Yenilmez E (2010) Release characteristics of vitamin E incorporated chitosan microspheres and in vitro–in vivo evaluation for topical application. Carbohydrate Polymers 84(2): 807-811.

22. Becerra EA, Otero YB, Manchado FC, Martínez FG, Massanet GM, et al. (2007) Synthesis and biological activity of epoxy analogues of 3-dehydroteasterone. Journal of Chemical Research 5: 268-271.

23. Quiñones JP, Coll Y, Curiel H, Covas CP (2010) Microspheres of chitosan for controlled delivery of brassinosteroids with biological activity as agrochemicals. Carbohydrate Polymers 80: 915-921.

24. David L, Domard A, Lucas JM, Madrazo AO, Peniche-Covas C P, et al. (2010) Kinetics Study of the Solid-State Acid Hydrolysis of Chitosan: Evolution of the Crystallinity and Macromolecular Structure. Biomacromolecules 11: 1376-1386.

25. Mau JL, Yang J, Yen MT (2009) Physicochemical characterization of chitin and chitosan from crab shells. Carbohydrate Polymers 75: 15-21.

26. El-Marakby EM, Hathout RM, Taha I, Mansour S, Mortada ND (2017) A Novel serum-stable liver targeted cytotoxic system using valerate-conjugated chitosan nanoparticles surface decorated glycyrrhizin. Int J Pharm 525(1): 123-138.

27. Kato Y, Ozawa S, Miyamoto C, Maehata Y, Suzuki A, et al. (2013) Acidic extracellular microenvironment and cancer. Cancer Cell Int 13: 1-8.

28. Duncan R, Richardson CW (2012) Endocytosis and intracellular trafficking as gateways for nanomedicine delivery: Opportunities and challenges. Molecular Pharmaceutics 9(9): 2380-2402.

29. Fan L, Li R, Pan J, Ding Z, Lin J (2015) Endocytosis and its regulation in plants. Trends Plant Sci 20(6): 388-397.

30. Salachna P, Zawadzinska A (2014) Effect of Chitosan on Plant Growth, Flowering and Corms Yield of Potted Freesia. Journal of Ecological Engineering 15(3): 97-102.

31. Liu J, Zhang D, Sun X, Ding T, Lei B, et al. (2017) Structure-activity relationship of brassinosterois and their agricultural practical usages. Steroids 124: 1-17.